Theoret. Chim. Acta (Berl.) 56, 93–112 (1980)

THEORETICA CHIMICA ACTA


# The Perturbation of a Polymer Molecular Orbital

David Antony Morton-Blake

Dept. of Chemistry, Trinity College, Dublin 2, Ireland

The symmetry restrictions imposed by the Born–Kármán boundary conditions on a polymer in order to calculate its electronic band structure are relaxed by the separate introduction of two types of perturbation at a site on the polymer chain. The first simulates a defect or the close approach of a molecule by modifying the segment orbital functions in the environment of the site while the second simulates a change in the distance between one pair of adjacent segments by altering the interaction between them. When applied to a molecular orbital described by a Bloch function and arbitrary energy band these perturbations generate a small number of electronic states whose energies lie above and below those of the band. The sign of the energy shift depends on the symmetry of the crystal orbital perturbed.

**Key words:** Polymer MOs – Perturbation of Bloch functions – Discrete states.

## 1. Introduction

Crystal orbital calculations on a polymer chain using Bloch functions and Born–Kármán boundary conditions [1] necessarily imply a crystal lattice possessing long-term order, i.e. translational symmetry, and for practical reasons must be confined to chains whose unit segments are not too large. As had also been done for (three dimensional) crystalline lattices [2] attempts were made recently to relax these symmetry restrictions by permitting the occurrence of certain internal rotations and bond alternations [3] or by creating chain ends in the Born–Kármán cyclic lattice [4] by a "perturbative rupture" of the polymer chain.

The result of such a symmetry lowering by reducing *short-term* order (e.g. through bond alternation or internal rotation [3]) is the creation or extension of band gaps and the general modifications of the energy bands of the "regular" or high-symmetry polymer chain. This conclusion follows from line-group symmetry considerations [5] (partly), from a direct calculation on the symmetry-lowered chain incorporating the extended unit segment [6], or

0040-5744/80/0056/0093/$04.00

alternatively from a perturbation calculation in which the distortion is introduced as a perturbation of the undistorted, high-symmetry wave functions [3]. If however the distortion is a non-periodic perturbation such as that involved in the rupture of the polymer chain [4] or in creating a crystal *surface* in the solid lattice the result on the energy band structure may be the formation of discrete levels ("surface states" in solid-state theory [7, 8]) in energy regions which would consist of "forbidden gaps" for the undistorted chain or lattice.

While the concept of "impurity" levels or other inter-band energy states which may exist for a crystalline lattice are of obvious importance and well-known in solid-state studies, the possibility of such states occurring for a polymer chain has not been so widely discussed. Since it seems reasonable to suppose that a polymer might undergo a *chemical reaction* at a symmetry-lowered or defect site in the chain, it would appear desirable to investigate the effect of such sites on the band structure in order to see whether the two possibilities mentioned – the formation or extension of band gaps, or the creation of discrete states – can be applied to the question of reactivity.

In order to develop a quantum chemical theory of polymers which has the possibility of including reactions, methods of calculation involving a perfect Born–Kármán cyclic lattice may have to be modified in order to take into account the important effects of chain defects or symmetry-lowered sites. Such sites exist statically in the solid state polymer and dynamically in solution. Because of the impracticability of working with a unit segment so enlarged as to include the desired defects a more tractable approach would be to subject the crystal orbital (Bloch molecular orbital) functions to the necessary perturbations.

In this paper a method is presented which introduces two types of perturbation centred at a particular site on a general polymer so as to affect a small number of chain segments. In Sects. 2 and 3 a perturbation alters the Coulomb integrals of these segments: in a real chain this might for example describe a lattice defect site or, in solution, the close approach of a reactant or solvent molecule. In Sect. 4 another type of perturbation is applied which modifies a single link between two segments so as to describe a bond compression or extension at this point.

## 2. Segment Perturbation: Theory

### *2.1. The Perturbation*

We propose to perturb a polymer chain by applying a potential $V$ which is centred at one of the chain segments $j$. It will be convenient to label this segment $j = 0$ so that positive and negative $j$ values label segments to the right and left of the perturbation site (Fig. 1).

As our set of zeroth order functions we shall use the one-dimensional

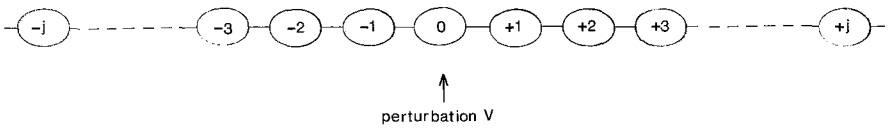


**Fig. 1.** The segment perturbation $V$ of a linear polymer, with $V$ centred on the segment $j=0$, the "perturbation site"

monoelectronic Bloch wave functions $\Psi^0(k)$ defined [1, 9] by

$$\Psi^0(k) = N^{-1/2} \sum_{j=0}^{\pm 1/2(N-1)} \exp(ijk)\chi_j \qquad (\text{odd } N, -\pi < k \leq \pi). \tag{1}$$

Employing the Born–Kármán boundary conditions Eq. (1) expresses the chain wave functions as a linear combination of the $N$ *segment* functions $\chi_j$ of the cyclic lattice. In this work it will be assumed that the set $\chi_j$ (which might, for example, consist of linear combinations of the atomic orbitals comprising the unit segment) has been calculated using some standard tight-binding computational method [9] applicable to a polymer chain. It will also be assumed for simplicity that the $\chi_j$ are mutually orthogonal; a relaxation of this restriction by admitting non-zero overlap integrals between the segment functions would result merely in the inclusion of a multiplicative factor of order unity in (1), and would not affect the conclusions of the work.

The monoelectronic functions defined by (1) will be taken to be eigenfunctions of an Extended-Hückel-type effective hamiltonian $H^0$ for the cyclic polymer chain, according to the equation

$$H^0\Psi^0(k) = E^0(k)\Psi^0(k)$$

This equation also defines an energy $E^0$ for each value of $k$, i.e. for each *microstate* $\Psi(k)$. The continuity of $k$ ensures that the ensemble of energy values $E^0(k)$ constitute an energy *band*. The mixing of the microstate wave functions $\Psi^0(k)$ due to the perturbation $V$ is now considered so as to give rise to new chain wave functions $\Psi_q^1$ which are expressible as linear combinations of $n$ orthogonal microstate functions:

$$\Psi_q^1 = \sum_{i=1}^{n} g_q(k_i)\Psi^0(k_i) \tag{2}$$

and which are eigenfunctions of the hamiltonian $H = H^0 + V$ of the perturbed system. $n$ is the number of states into which we conveniently divide up the Brillouin zone for the purpose of the calculation. It is to be distinguished from $N$ which is the true, practically infinite, number of microstates constituting the Brillouin zone, and which renders $k$ ($=2\pi p/N$, where $p$ is an integer between $-\frac{1}{2}N$ and $+\frac{1}{2}N$) a continuous variable. The states described by (2), generated by the perturbation, may be either discrete, or, like the set $\Psi^0(k_i)$, quasi-continuous.

From (1) the general element $V(k_1, k_2)$ of the Bloch MO perturbation matrix is

given by

$$V(k_1, k_2) = \int \Psi^{0*}(k_1) V \Psi^0(k_2)\, d\tau$$

$$= n^{-1} \sum_{j_1=0}^{\pm} \sum_{j_2=0}^{\pm} \exp(-ij_1k_j) \exp(ij_2k_2) \int \chi_{j_1}^* V \chi_{j_2}\, d\tau$$

$$V(k_1, k_2) = n^{-1} \sum_{j_1=0}^{\pm} \sum_{j_2=0}^{\pm} \exp(-ij_1k_1) \exp(ij_2k_2) V_{j_1j_2}$$

where $V_{j_1j_2}$, the general element of the segment orbital perturbation matrix, is the *change* in the value of the integral $\int \chi_{j_1}^* H^0 \chi_{j_2}\, d\tau$ (expressing the interaction between segments $j_1$ and $j_2$) when the perturbation is applied. The $\pm$ symbols over the sigmas indicate summations over positive and negative $j$'s up to the same formal limits as in (1), however because of the convergence of the series only few terms need be considered.

We shall perturb the polymer wave function through the coulomb terms $\int \chi_j^* H \chi_j\, d\tau$ of the segment orbitals. The segment orbital at $j = 0$ will be perturbed the most; the pair in the $j = \pm 1$ segments come next, to be followed by those in $j = \pm 2$, etc. It is proposed that the segment perturbation term $V_{j_1j_2}$ can be represented as the product of two equivalent functions $u(j_1)$ and $u(j_2)$ whose values diminish with increasing displacement $|j|$ from the perturbation site at $j = 0$. Thus $V_{j_1j_2}$ would then as required be greatest when both segments involved are in the vicinity of the perturbation ($j_1 \simeq j_2 \simeq 0$) and diminish as the interactions of progressively more distant elements are considered. We therefore write $V_{j_1j_2} = vu^*(j_1)u(j_2)$ where $v(\equiv V_{00})$ is the *amplitude* of the perturbation if $u(j)$ is scaled so that $u(0) = 1$. This allows the summations in $V(k_1, k_2)$ to separate into two equivalent functions of $k$:

$$V(k_1, k_2) = \frac{v}{n} \sum_{j=0}^{\pm} \exp(-ijk_1) u^*(j) \sum_{j=0}^{\pm} \exp(ijk_2) u(j)$$

$$V(k_1, k_2) = \frac{v}{n} W^*(k_1) W(k_2) \tag{3}$$

where

$$W(k) = \sum_{j=0}^{\pm} \exp(ijk) u(j) = 1 + 2 \sum_{j=1}^{+} u(j) \cos jk. \tag{4}$$

The perturbation is assumed to be symmetric, so that $u(j) = u(-j)$, when the $\pm j$ summation can be replaced by one involving positive $j$ only.

A natural concern at this stage is whether the practical consideration of limiting $n$ to a finite value (rather than using the practically infinite quantity $N$ usually implied in the Bloch function (1) might invalidate the calculation proposed. We shall see that as $n$ – the number of microstates selected to interact along the band – is increased, the $1/n$ factor in the $V(k_1, k_2)$ expression (3) produces quite a rapid convergence, thus permitting the use of a manageable number of microstates.

### 2.2. *The Unperturbed Energy Band*

The energy matrix $\boldsymbol{H}$ to be diagonalized is composed of the diagonal matrix $\boldsymbol{E}^0$ – consisting of the band energies $E^0(k_i)$ of the microstates $\Psi^0(k_i)$ – and of the Bloch function perturbation matrix $\mathbf{V}$ whose elements we have discussed:

$$\boldsymbol{H} = \boldsymbol{E}^0 + \mathbf{V}. \tag{5}$$

In order to perform a perturbation calculation of the kind developed here we shall find it convenient to assume a hypothetical function to describe the unperturbed energy band $E^0(k)$. The simplest type of band meeting the necessary conditions

$$\left(\frac{dE^0(k)}{dk}\right)_{k=0} = \left(\frac{dE^0(k)}{dk}\right)_{k=\pm\pi} = 0$$

and

$$E^0(k) = E^0(-k)$$

is one having the dispersion equation

$$E^0(k) = E^0 + E_w \sin^2 \tfrac{1}{2}k.$$

Since the constant reference energy term $E_0$ would appear only in the diagonal elements of $\boldsymbol{H}$ its only effect would be to shift the eigenvalues by the same amount, $E_0$. The term is therefore irrelevant to the perturbation and can be omitted; the resulting energy band expression generating the $\boldsymbol{E}^0$ matrix is thus

$$E^0(k_i) = E_w \sin^2 \tfrac{1}{2}k_i \tag{6}$$

where $k_i$ is the value of the $i^{\text{th}}$ microstate and $|E_w|$ the width of the energy band. The sign of $E_w$ determines whether the dispersion energy function has a minimum or a maximum at the centre ($k = 0$) or at the edges ($k = \pm\pi$), of the Brillouin zone.

### 2.3 *Results of the Perturbation*

Before embarking on the numerical calculations we can already make some useful qualitative predictions about the results. When the microstate $\psi^0(k_1)$ is perturbed in the presence of all the others its energy, taken to 2nd order, is given by

$$E(k_1) = E^0(k_1) + V(k_1, k_1) + \sum_{k_2}{}' \frac{|V(k_1, k_2)|^2}{E^0(k_1) - E^0(k_2)}, \tag{7}$$

the elements $V(k_1, k_2)$ being given by Eqs. (3) and (4). Now the combined effect of the destructive interference of the $\cos jk$ factor in (4) and of the attenuating nature of the $u(j)$ function is to make $W(k)$ largest for $k = 0$. Consequently the most significant elements $V(k_1, k_2)$ in (7) are those derived from microstates $\psi^0(k)$ at the centre of the Brillouin zone. However from the condition $E^0(k_j) = E^0(-k_j)$, we see that the 2nd order correction to the energy

of $\psi^0(k=0)$ vanishes since the summation in (7), running over positive and negative $k_j$ values, generates mutually cancelling terms.

In short the effect of the perturbation is to shift the energies of the microstates which are close to $k=0$. The direction of the shift depends on the sign of $V$ in the region of the segments which are the most affected. Using the representation implied by Eqs. (3) and (4) we would expect a potential of positive amplitude $v$ to produce upward-displaced energy states, while if $v<0$ the perturbation energies would be negative. This also implies that the new states resulting from a positive potential perturbing a $\psi^0(k)$ band with a positive $E_w$ in (6) would not be pronounced, and might not even be distinguishable at all: for a band with a minimum at $k=0$ any perturbation state produced above the band would, for small perturbations, have to derive from $\psi^0(k)$ microstates for which $k \simeq \pi$ which, we have just argued, gives rise to *small* $V(k_1, k_2)$ elements. (A small perturbation of $\psi^0(k=0)$ would shift it into an energy region already occupied by microstates.) The creation of discrete perturbation states from a $E^0(k)$ band with a minimum at $k=0$ can most easily be achieved with a *negative* $V$ potential, while conversely those from a band with a maximum at $k=0$ could be created from a *positive* $V$ potential.

The complementarity of the signs of $E_w$ and of $v$ may be seen from (5): reversing the signs of both $\boldsymbol{E}^0$ (which would result from replacing $E_w$ by $-E_w$) and $\boldsymbol{V}$ would produce a matrix $-\boldsymbol{H}$ whose eigenvalues are just the negative of those of $\boldsymbol{H}$. The effect of the sign changes is thus to move the perturbation states from one side of the $E^0(k=0)$ level to the other.

### 2.4. Real Orbital Wave Functions

It is useful to exploit the chain symmetry element relating segments on either side of the perturbation site at $j=0$. This is because practical considerations restrict us to a finite value for $n$, and so the application of symmetry might permit a more judicious choice of microstates to represent the band.

Additive and subtractive combinations of the (degenerate) Bloch MOs for $k$ and $-k$ defined in (1), namely

$$\Psi^0_{\pm}(k) = \frac{1}{\sqrt{2}}[\Psi^0(k) \pm \Psi^0(-k)] \qquad (0 \leqslant k \leqslant \pi), \tag{8}$$

result in the real chain orbital functions

$$\Psi^0_{\pm}(k) = \sqrt{\frac{Z(k)}{N}} \sum_{j=0}^{+1/2(N-1)} \chi_j \operatorname{cs}(jk) \qquad (0 \leqslant k \leqslant \pi) \tag{9}$$

where cs means "cosine" if the combination is additive ($\Psi^0_+$) and "sine" if it is subtractive ($\Psi^0_-$). Because of the $k$ range defined in (1) the combination (8) does not couple positive with negative $k$ values when $k=0$ or $k=\pi$; hence in (9) the symbol $Z(k)$ means "1" if $k$ is 0 or $\pi$ and "2" in all other cases.

Since $V$ is declared to be a symmetric perturbation [$V(j)=V(-j)$] it will not

mix $\Psi_+^0$ with $\Psi_-^0$ states – we can therefore consider these two symmetry cases separately. With the same relationship between "±" and "cs" as in (9) the perturbation relationships corresponding to those in (3) and (4) are:

$$V_\pm(k_1, k_2) = \frac{\sqrt{Z(k_1)Z(k_2)}}{n} W^*(k_1) W(k_2) \tag{10}$$

and

$$W_\pm(k) = \sum_{j=0}^{\pm} u(j) \operatorname{cs}(jk). \tag{11}$$

But if $V$ is symmetric in $j$ the distribution function $u(j)$ will also be. Then of the two types of function defining $W_+$ and $W_-$ in (11) only the *cosine* function $W_+$ will give rise to a non-zero perturbation matrix since $W_-$ will consist of the mutually cancelling pairs of terms $u(j)\sin(jk) + u(-j)\sin(-jk)$. We need therefore consider only the function $\Psi_+^0(k)$ defined by

$$\Psi_+^0(k) = \sqrt{\frac{Z(k)}{n}} \sum_{j=0}^{\pm} \chi_j \cos(jk) \tag{12}$$

which gives rise to the general perturbation matrix

$$V_+(k_1, k_2) = v \frac{\sqrt{Z(k_1)Z(k_2)}}{n} \left[1 + \sum_{j=1}^{+} u(j) \cos(jk_1)\right] \times \left[1 + \sum_{j=1}^{+} u(j) \cos(jk_2)\right]. \tag{13}$$

In (12) and (13) $n$ is still the number of *basic* Bloch wave functions $\Psi^0(k)$ defined in (1) that are being combined. But since the basic microstates (8) now being considered consist of symmetry-reduced functions each of which is derived from a $\Psi^0(k)$ and $\Psi^0(-k)$ *pair*, $n$ will be about twice the number of $\Psi_+(k)$ states in the calculation, allowance being made for the unique $k = 0$ and $k = \pi$ states if included.

## 3. Numerical Results

In a preliminary series of calculations the number of microstate wave functions used to represent the energy band was varied (for different conditions of amplitude, exponent and band width) to investigate the convergence of the results with respect to $n$ in (13). It was found that for most of the conditions considered, convergence, as decided by the energy $\varepsilon$ of the discrete "perturbation" level (see Sect. 3.1), was complete by $n = 16$, though in a small number of cases an $n$ value of 20 had to be used to achieve this. In order to ensure confidence in the convergence of subsequent calculations a value of 30 was uniformly used, except in the "sample calculation" of Sect. 3.1 where, so as to display results adequately for the purpose of discussion, the smaller value $n = 16$ (nine $\Psi_+^0(k)$ microstates] was used. In fact convergence was almost

achieved even in this case – the reported discrete energy level $\varepsilon = 0.7028$ eV changes only to 0.7022 eV at complete convergence, thus validating the use of this calculation to represent the features of the subsequent investigations.

### *3.1. Sample Calculation*

The matrix $\boldsymbol{H}$ to be diagonalised, defined by Eqs. (5), (6) and (13), was constructed using the real microstate wave functions (12). $E_w$ was assigned a value of $-10$ eV, the sign indicating a $E^0(k)$ curve with a maximum at the centre of the Brillouin zone. The band was perturbed by a potential $V$ in which the function $u(j)$ appearing in (13) was defined by the Gaussian form

$$u(j) = u(0) \exp(-aj^2) \tag{14}$$

where $u(0) = 1$, and the amplitude $v$ of the perturbation chosen as 2.0 eV. The exponent $a$ in (14) was put equal to 2. Note that such a $u(j)$ function gives the necessary symmetric perturbation function $V(j)$, and that the chosen value of the exponent in this case indicates a highly localized perturbation site of just one or two segments.

The elements of the perturbation matrix $\mathbf{V}$ (Table 1) reflect the observations made in Sect. 2.3, namely, that the most significant elements are those for $k_1$ and $k_2$ close to zero. (The apparently smaller values for the elements involving the $k = 0$ state occur because the $Z$ value [Sect. 2.4] of such a state is half that of the other states since we are using symmetry-reduced basis functions.)

The result of the diagonalization of $\boldsymbol{H}$ is to produce a spectrum of energy eigenvalues $E_q^1$ which, with one exception, lie within the range of the unperturbed $E^0(k)$ energy band, 0 to $-10$ eV. In fact if the $E_q^1$ values were plotted against their "effective $k$ values"

$$k_q^{\text{eff}} = \sum_i |g_q(k_i)|^2 \, k_i, \tag{15}$$

the points, except that for the high-energy state at $E_{q^*}^1 = +0.7028$ eV, would lie very close to the curve of the $E^0(k)$ function, as we shall see in Sect. 3.2. The symbol $q^*$ will be used to label such *discrete states* as this one. $E_{q^*}^1$ is separated by an energy gap $\varepsilon = 0.7028$ eV from the nearest $E^0(k)$ microstate, and also by an almost equal gap from the nearest of the remaining perturbed band state energies $E_q^1$. The nature of this discrete state is also revealed by its eigenvectors $g_{q^*}(k)$. Table 1 shows that the coefficients of the "normal" quasi-continuous states are strongly peaked at some particular $k$ value so that $|g_q(k)| > 0.9$, the contributions from the remaining microstates being very small. The coefficients of the higher two perturbation states are peaked less strongly, and at low $k$ values. In other words, while each of the "normal" states is essentially an unperturbed microstate $\Psi_+^0(k)$ of the band, the upper two contain a significantly greater admixture of other microstates. However, of these states only one constitutes a discrete level.

**Table 1.** Sample calculation for segment perturbation $V$ with $v = 2$ eV, $E_w = -10$ eV, $a = 2$ and $n = 16$ (See Sect. 3.1)

(a) Energies $E^0(k)$ of selected unperturbed microstates (eV) and the energy matrix

| $k$ | $E^0(k)$ | $k$: | 0.0000 | 0.3927 | 0.7854 | 1.1781 | 1.5708 | 1.9635 | 2.3562 | 2.7489 | 3.1416 |
|---|---|---|---|---|---|---|---|---|---|---|---|
| 0.0000 | 0.0000 | | 0.202 | | | | | | | | |
| 0.3927 | −0.3806 | | 0.281 | 0.010 | | | | | | | |
| 0.7854 | −1.4645 | | 0.268 | 0.372 | −1.109 | | | | | | |
| 1.1781 | −3.0866 | | 0.248 | 0.345 | 0.329 | −2.782 | | | | | |
| 1.5708 | −5.0000 | | 0.225 | 0.312 | 0.298 | 0.276 | −4.750 | | | | |
| 1.9635 | −6.9134 | | 0.201 | 0.280 | 0.267 | 0.247 | 0.224 | −6.712 | | | |
| 2.3562 | −8.5355 | | 0.182 | 0.253 | 0.241 | 0.223 | 0.202 | 0.181 | −8.372 | | |
| 2.7489 | −9.6194 | | 0.169 | 0.235 | 0.223 | 0.207 | 0.187 | 0.168 | 0.152 | −9.478 | |
| 3.1416 | −10.0000 | | 0.116 | 0.161 | 0.154 | 0.142 | 0.129 | 0.116 | 0.104 | 0.097 | −9.933 |

(b) Energy eigenvalues $E_q^1$, effective $k$ values and eigenvectors $g_q(k)$

| $E_q^1$ | $k_q^{\text{eff}}$ | $k$: | 0.0000 | 0.3927 | 0.7854 | 1.1781 | 1.5708 | 1.9635 | 2.3562 | 2.7489 | 3.1416 |
|---|---|---|---|---|---|---|---|---|---|---|---|
| 0.7028 | 0.286 | | 0.692 | 0.625 | 0.298 | 0.158 | 0.095 | 0.061 | 0.047 | 0.039 | 0.026 |
| −0.1595 | 0.209 | | −0.700 | 0.703 | 0.113 | 0.047 | 0.026 | 0.017 | 0.012 | 0.010 | 0.006 |
| −1.1992 | 0.739 | | −0.155 | −0.315 | 0.926 | 0.121 | 0.054 | 0.032 | 0.023 | 0.018 | 0.012 |
| −2.8456 | 1.159 | | −0.067 | −0.107 | −0.182 | 0.968 | 0.098 | 0.047 | 0.030 | 0.023 | 0.015 |
| −4.7977 | 1.561 | | −0.037 | −0.056 | −0.071 | −0.128 | 0.981 | 0.084 | 0.043 | 0.031 | 0.020 |
| −6.7494 | 1.957 | | −0.024 | −0.035 | −0.041 | −0.054 | −0.103 | 0.986 | 0.081 | 0.047 | 0.029 |
| −8.4028 | 2.352 | | −0.017 | −0.025 | −0.028 | −0.034 | −0.047 | −0.097 | 0.986 | 0.100 | 0.052 |
| −9.5126 | 2.746 | | −0.013 | −0.019 | −0.021 | −0.024 | −0.031 | −0.048 | −0.115 | 0.980 | 0.148 |
| −9.9627 | 3.129 | | −0.006 | −0.009 | −0.010 | −0.011 | −0.014 | −0.021 | −0.040 | −0.156 | 0.986 |

An implication of the $g(k)$ distribution is seen if we write the perturbed state wave function, using (1) and (2) as follows:

$$\Psi_q^1 = N^{-1/2} \sum_i^N g_q(k_i) \sum_j^N \exp(ijk_i)\chi_j$$

$$\rightarrow N^{-1/2} \sum_j^N \left[ \int g_q(k) \exp(ijk)\, dk \right] \chi_j \qquad \text{as } N \rightarrow \infty \tag{16}$$

(or the corresponding real form). Clearly the "broader" the $g(k)$ distribution – i.e. the more $\Psi^0(k)$ states are mixed in to form $\Psi_q^1$ – the smaller will be the value of the square-bracketed Fourier transform integral in (16) for segments other than $j \sim 0$. But since this quantity is the coefficient of the $j^{\text{th}}$ segment in the perturbed orbital, the effect of $V$ in creating the discrete states is to *localize* the wave function $\Psi_{q*}^1$ at the perturbation site.

### *3.2. Variation of the Perturbation*

The same energy band as that used in the previous section was perturbed by a potential giving rise to $V(k_1, k_2)$ elements again calculated by (13) and (14). The shape of the potential function was varied by changing its *amplitude* $v$, and also its *extent* by the use of different values $a$ as exponent in (14). The results are shown in Fig. 2, where the curve is that of the unperturbed energy band function $E^0(k)$ given by (6) with $E_w = -10$ eV. The microstates $\Psi_+^0(k_i)$ selected by dividing the Brillouin zone into 30 points are shown by the 16 points (**X**) on the energy curve. The circled points are the eigenvalues $E_q^1$ of $\boldsymbol{H}$ plotted against their $k_q^{\text{eff}}$ values as defined in (15).

Increasing the perturbation amplitude has the effect of increasing the separation $\varepsilon$ of the "discrete" perturbation level from the band while leaving the remaining states almost as unperturbed microstates $\Psi_+^0(k_i)$. So as to avoid complicating the diagram, which is intended primarily to show the discrete perturbation levels $E_{q*}^1$, the non-discrete or quasi-continuous energies $E_q^1$ only for the "most perturbed" conditions are plotted in Fig. 2 – those corresponding to $v = +10$ eV and $a = 0.25$; the rest would lie even closer to the $E^0(k)$ curve. As expected the points tend to coincide with those of the unperturbed microstates as we leave the $k \sim 0$ region.

The same trend as that resulting from increasing $v$ is followed when the $V$ function is broadened by reducing the exponent $a$. If we use the quantity $\sum_j^{\pm} e^{-aj^2}$ to measure the number of segments affected by the perturbations considered we find 1.1 segments for $a = 3$, 1.8 for $a = 1$ and 3.5 for $a = 0.25$: there is clearly a sharp rise in the $\varepsilon$ values as the number of perturbed segments increases.

The discrete states derived from a negative perturbation potential ($v < 0$) have smaller $\varepsilon$ values than those for $v > 0$, as expected from the discussion in Sect. 2.3. Figure 2 shows that for small perturbations these states derive mainly from $\Psi_+^0(k)$ microstates with $k$ in the region of $\pi$ (which naturally produce small

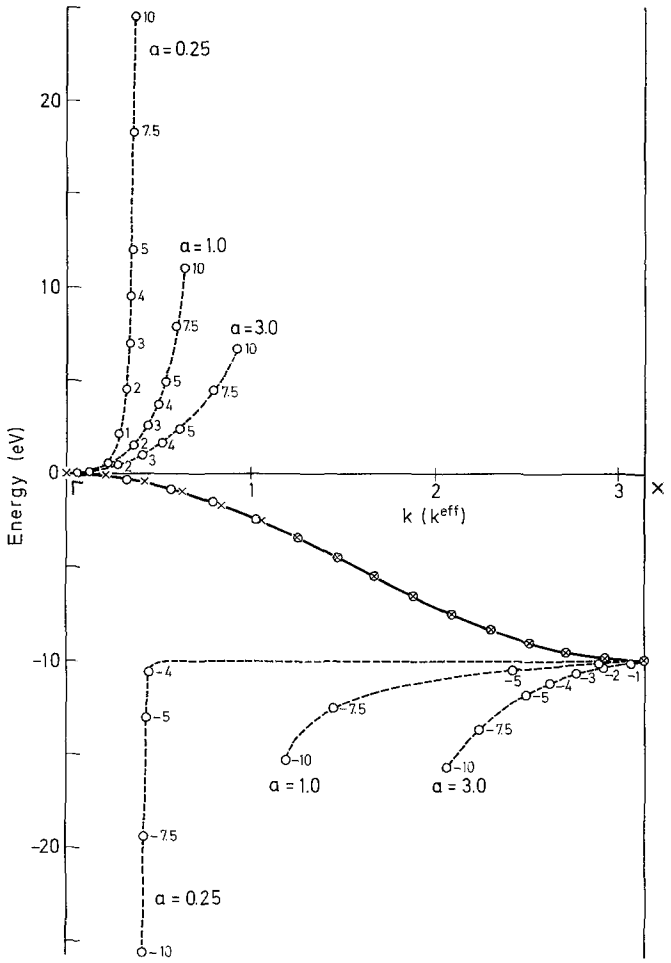


**Fig. 2.** The application of the segment perturbation $V$ to a 10 eV energy band $E^0(k)$ (continuous curve), with various perturbation amplitudes $v$ (−10 to +10 eV) and exponents $a$

separations $\varepsilon$). As $-v$ increases, however, $\boldsymbol{H}$ in (5) eventually becomes dominated by its component $\boldsymbol{V}$ so that the perturbation states $\Psi^1_{q*}$ receive greater contributions from $\Psi^0_+(k)$ microstates near the centre of the Brillouin zone.

### *3.3. Variation of the Width $E_w$ of the Energy Band*

With the exponent fixed at $a = 1$ $E_w$ was varied from −20 to +20 eV; in this way the behaviour of the two types of band referred to in Sects. 2.2 and 2.3 – maximum at $k = 0$ and minimum at $k = 0$ – was investigated. Figure 3 shows how the separation of the discrete level $\varepsilon$ from the band varies with the width $E_w$ of the two band types – those with $E_w < 0$ and $E_w > 0$ respectively.

As we would expect – for example from (7) – the narrower the band the larger

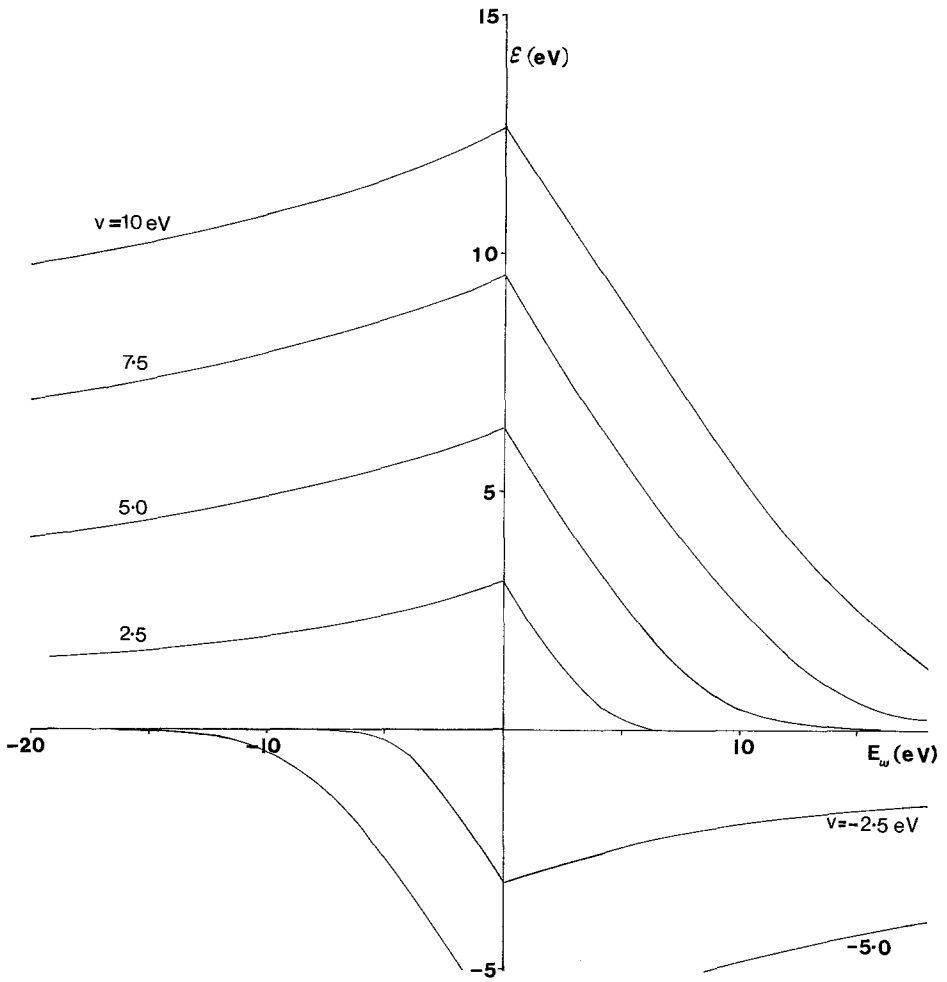


**Fig. 3.** The separation $\varepsilon$ of the $V$-generated "discrete levels" from the energy band of various widths $E_w$ and for various amplitudes $v$

the value of $\varepsilon$, and as seen in Sects. 2.3 and 3.2 a positive perturbation produces a greater effect on bands with a maximum at $k=0$ ($E_w<0$ region of Fig. 3) than on those with a minimum at $k=0$ ($E_w>0$ region). Naturally the converse is true for the negative perturbations ($v<0$) and so the family of curves ($v=-2.5$, $-5.0$, etc.) can be obtained by inverting the corresponding positve-$v$ curve through the origin. The $\varepsilon$ value tends to a proportionality with $v$ for narrow energy bands and increases more rapidly with $v$ for large $|E_w|$ values.

### *3.4. Step Potential*

Instead of the function (14) which describes a perturbation with a maximum effect at one segment and which diminishes with increasing distance from this

point, we could consider one which exerted the *same* influence on a specified number of different segments. Such a step function could be defined by the conditions

$$\left.\begin{array}{ll} u(j)=1 & \text{for } j=0,\pm1,\ldots,\pm m \\ \text{and} & \\ u(j)=0 & \text{for all other segments} \end{array}\right\} \tag{17}$$

A potential derived from this function would simplify the matrix element expression (13) by omitting the factor $u(j)$ in the summands and by including just the $j$ segments 1 to $m$ in the summations.

The results of applying such a perturbation to the $2m+1$ adjacent segments implied by (17) are broadly similar to those discussed using the gaussian function (14). Indeed. if we compare the $\varepsilon$ values obtained using the function (14) of the same width (which would be $\sum_{j=0}^{\pm} e^{-aj^2}$ for the Gaussian, as in Sect. 3.2, and $2m+1$ for the step function) and amplitude $v$, the results (Table 2) are

**Table 2.** Discrete-level separation energies $\varepsilon$ (eV) as calculated by a Gaussian (Eq. 14) and by a step function (Sect. 3.4) form for $u(j)$ and their dependence on the widths of the perturbation. Other data: $E_w = -10$ eV, $v = 2$ eV

| Gaussian $u(j)$ | | | Step function $u(j)$ | |
|---|---|---|---|---|
| $a$ | width[a] | $\varepsilon$ | width | $\varepsilon$ |
| 7.5 | 1.00 | 0.39 | 1 | 0.39 |
| 0.35 | 2.99 | 3.61 | 3 | 4.84 |
| 0.126 | 4.99 | 6.78 | 5 | 9.25 |
| 0.064 | 7.01 | 9.76 | 7 | 13.44 |

[a] See Sect. 3.4

at least of the same order and become more nearly equal as the widths decrease towards unity. This suggests that apart from the parameters $v$ and $w$ the perturbation results are not very sensitive to the finer details of the $V$ function, particularly if the potential is a "narrow" one.

## 4. Chain Link Distortion Perturbation

### *4.1. Theory*

In this section we consider a polymer chain subjected to a perturbation $V'$ which distorts a single chain link. In order to express $V'$ consider a plane boundary intersecting the circular polymer chain between segments $j=1$ and $j=N$ which of course are adjacent (Fig. 4). Then $V'$ acts on the polymer by modifying the interactions between segments on opposite sides of the boundary. As in Sect. 2 we shall suppose that the effect of $V'$ on the chain functions $\Psi^0(k)$ can be obtained by constructing the perturbation matrix $\mathbf{V}'$ and

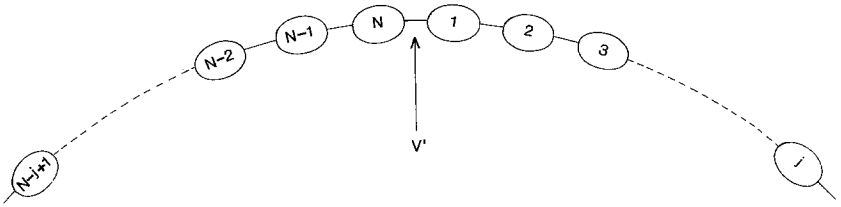


**Fig. 4.** The definition of the single link distortion perturbation $V'$ applied between the segments $j=1$ and $j=N$

diagonalizing the resulting energy matrix $\boldsymbol{H}$ as was done for the matrix expressed in (5).

We shall now write the real microstate functions $\Psi_+^0(k)$ as

$$\Psi_{\pm}^0(k)=\sqrt{\frac{Z(k)}{N}}\sum_{i=1}^{N}\chi_i \operatorname{cs}(i-\tfrac{1}{2})k \qquad \begin{cases}0\leqslant k<\pi\\ 0<k\leqslant\pi\end{cases} \tag{18}$$

rather than as (9) in order that they reflect the symmetry of Fig. 4 which has a mirror plane between segments $j=1$ and $j=N$. Notice that, unlike the limits declared in (8), the $k$ range of the cosine function $\Psi_+^0$ does not include the point $k=\pi$.

The general element of $\mathbf{V}'$ expressing the perturbative interaction between $k_1$ and $k_2$ is now

$$\begin{aligned}V'_{\pm}(k_1,k_2)&=\frac{\sqrt{Z(k_1)Z(k_2)}}{N}\int\left[\sum_{i=1}^{N}\chi_i \operatorname{cs}(i-\tfrac{1}{2})k_1\right]^{*}V'\left[\sum_{i=1}^{N}\chi_i \operatorname{cs}(i-\tfrac{1}{2})k_2\right]d\tau\\ &=\frac{\sqrt{Z(k_1)Z(k_2)}}{N}\sum_{i_1,i_2=1}^{N}V'_{i_1i_2}\operatorname{cs}(i_1-\tfrac{1}{2})k_1 \operatorname{cs}(i_2-\tfrac{1}{2})k_2\end{aligned} \tag{19}$$

where

$$V'_{i_1i_2}=\int \chi_{i_1}^{*}V'\chi_{i_2}\,d\tau$$

is the *change* in the interaction between segments $i_1$ and $i_2$ on opposite sides of the boundary when the perturbation is applied. Again "cs" means cosine or sine according to the choice of upper or lower sign in $\pm$ respectively. Clearly the greatest contribution to $V'$ will be from $V'_{1,N}$, which is the change suffered by the integral $\int \chi_1^{*}H\chi_N\,d\tau$ expressing the interaction between segments 1 and $N$; the next largest will be $V'_{2,N}=V'_{1,N-1}$, followed by $V'_{3,N}=V'_{1,N-2}$, etc. It should also be obvious that the magnitudes of the elements $V'_{i_1,i_2}$ diminish rapidly along such a series which, however, is not the natural order of $i_2$.

We therefore replace the labels $i_1$ and $i_2$ by the pair $j_1$ and $j_2$ which count the segments in opposite directions, starting at $i=1$ and $i=N$ respectively (see Fig. 4). Then the new labels are defined by

$$\left.\begin{aligned}&j_1=i_1\\ \text{and}\quad&\\ &j_2=N+1-i_2\end{aligned}\right\}. \tag{20}$$

We wish to simulate a perturbation with the effect described by modifying the $H_{j_1 j_2}$ elements[1] through a component $V'_{j_1 j_2}$. Then the largest $V'_{j_1 j_2}$ quantity will be that for $j_1 = j_2$ and the other elements will decrease with increasing $j_1 + j_2$. We propose the relation

$$V'_{j_1 j_2} = v' e^{-aj} \tag{21}$$

where

$$j = j_1 + j_2 - 2 \tag{22}$$

is a measure of the separation of the segments on either side of the boundary; the quantity $v'$, which is analogous to $v$ in Sect. 2.1, will similarly be termed the "amplitude" of the perturbation since it denotes the element of greatest magnitude, $V'_{11}$.

Transforming (19) according to (20) and (21) we get

$$V'_{\pm}(k_1, k_2) = v' \frac{\sqrt{Z(k_1)Z(k_2)}}{N} \sum_{j_1, j_2 = 1}^{N} \operatorname{cs}([j_1 - \tfrac{1}{2}]k_1) \operatorname{cs}([\tfrac{1}{2} - j_2]k_2) e^{-aj}.$$

Although we pointed out the rapid decay of $V'_{j_1 j_2}$ as $j_1$ and $j_2$ progress along the series 1, 2, 3, etc. it must be remembered that as the $j$'s approach $N$ they give rise to $V'_{j_1 j_2}$ terms similar to those for small $j_1$ and $j_2$. The terms resulting from the replacement of $j_1$ and $j_2$ by $N - j_1$ and $N - j_2$ will be written separately with the $j$'s extending over just the small values required for convergence:

$$V'_{\pm}(k_1, k_2) = v' \frac{\sqrt{Z(k_1)Z(k_2)}}{N} \sum_{j_1, j_2 = 1}^{\text{small}} [\operatorname{cs}(j_1 - \tfrac{1}{2})k_1 \operatorname{cs}(\tfrac{1}{2} - j_2)k_2 + \operatorname{cs}(\tfrac{1}{2} - j_1)k_1 \operatorname{cs}(j_2 - \tfrac{1}{2})k_2] e^{-aj}.$$

Using (22) to replace the summation over $j_2$ by one $\sum(j)$ depending on just the separation of the segments across the boundary we have, for the + and − states:

$$V'_{+}(k_1, k_2) = \frac{2v'}{n} \sqrt{Z(k_1)Z(k_2)} \left[ \sum_{j_1 = 1}^{\text{small}} \cos(j_1 - \tfrac{1}{2})k_1 \cos(j_1 - \tfrac{3}{2})k_2 \times \sum_{j = j_1 - 1}^{\text{small}} e^{-aj} \cos jk_2 + \sum_{j_1 = 1}^{\text{small}} \cos(j_1 - \tfrac{1}{2})k_1 \sin(j_1 - \tfrac{3}{2})k_2 \sum_{j = j_1 - 1}^{\text{small}} e^{-aj} \sin jk_2 \right] \tag{23}$$

and

$$V'_{-}(k_1, k_2) = \frac{2v'}{n} \sqrt{Z(k_1)Z(k_2)} \left[ \sum_{j_1 = 1}^{\text{small}} \sin(j_1 - \tfrac{1}{2})k_1 \sin(j_1 - \tfrac{3}{2})k_1 \sum_{j = j_1 - 1}^{\text{small}} e^{-aj} \cos jk_2 - \sum_{j_1 = 1}^{\text{small}} \sin(j_1 - \tfrac{1}{2})k_1 \cos(j_1 - \tfrac{3}{2})k_2 \sum_{j = j_1 - 1}^{\text{small}} e^{-aj} \sin jk_2 \right]. \tag{24}$$

[1] A strict transformation of labels would of course take $H_{i_1 i_2}$ into $H_{i_1, N+1-i_2}$; however we shall shun the inelegance of such subscripts and write $H_{j_1 j_2}$ and $V'_{j_1 j_2}$.

As in (3) and (13) $N$ has been replaced by $n$ since we are limited to a finite number of microstates.

### 4.2. *Microstates Affected by $V'$*

An examination of the expressions (23) and (24) defining the matrix elements of $\mathbf{V}'$ and for the + and − functions (18) reveals that the microstates $\Psi^0_{\pm}(k=0)$ which are likely to be the most perturbed by $V'$ are $\Psi^0_{\pm}(k=0)$ and $\Psi^0_{-}(k=\pi)$; those corresponding to the other $k$ values are subject to a "destructive interference" by successive $j$-segments, similar to that referred to in Sect. 2.3 for the $V(k_1, k_2)$ terms. Unlike the case of the chain segment perturbation $V$ discussed in Sects. 2 and 3 therefore, we must now retain both $\Psi^0_{\pm}$ and $\Psi^0_{-}$ functions to investigate the possible creation of discrete states by the chain link distortion perturbation $V'$. Moreover (23) and (24) predict energy shifts from the band energies at $k=0$ and $k=\pi$ *in opposite directions* to give rise to possible discrete states derived from $\Psi^0_{+}(k=0)$ and $\Psi^0_{-}(k=\pi)$.

As in the previous sections the directions of the perturbative shifts sustained by $\Psi^0_{+}(k=0)$ and $\Psi^0_{-}(k=\pi)$ depend on the sign of the amplitude of the perturbation, $v'$. For $v'>0$, corresponding to an extension of the link between segments $j=1$ and $j=N$ (Fig. 4), $\Psi^0_{+}(k=0)$ is displaced upwards and $\Psi^0_{-}(k=\pi)$ downwards, though the requirement that $E^0(k=0)$ be a maximum and $E^0(k=\pi)$ a minimum (Sect. 2.3) is of course valid also here. We shall again assume the band dispersion relationship (6) with $E_w$ (usually) negative so that the band has a maximum at the centre, and minimum at the edges, of the Brillouin zone, but shall bear in mind the complementarity of this model with that in which the band maximum and minimum are reversed and in which $v$ is negative.

We can summarize the observations made in the previous paragraph as follows. A polymer chain subjected to an *extension* at one inter-segment link may give rise to discrete states $\Psi^1_{q*}$ both above and below the unperturbed band provided the band is one with a maximum at the centre, and minimum at the edges, of the Brillouin zone. A *compression* of the polymer at one segmental link, on the other hand, would not necessarily be expected to produce discrete states, at least for small or moderate amplitudes $|v'|$ of compression, but might generate such states from energy bands which have a minimum at the centre, and maximum at the edges, of the Brillouin zone.

### 4.3. *Numerical Results*

Just as in the segment perturbations of Sects. 2 and 3, a series of preliminary calculations established that the computed special states $\Psi^1_{q*}$ and their energies $E^1_{q*}$ were independent of the division of the Brillouin zone into a finite number ($n$) of microstates, and that increasing $n$ beyond 16 or 20 had negligible effect on the results. With the exception of the "sample calculation" to be reported for illustration purposes the value of $n$ was consequently again set at 30 in order to ensure convergence.

**Table 3.** Sample calculation [Energies $E_q^1$, effective $k$-values and eigenvectors $g_q(k)$] for link perturbation $V'$ with $v' = \text{lev}$, $E_w = -10$ eV and $n = 16$. (see Sect. 4.3)

(a) "cosine" states $\Psi_+^0$

| $E_q^1$ | $k_q^{\text{eff}}$ | $k$: 0.0000 | 0.3927 | 0.7854 | 1.1781 | 1.5708 | 1.9635 | 2.3562 | 2.7489 |
|---|---|---|---|---|---|---|---|---|---|
| 0.4019 | 0.167 | 0.800 | 0.555 | 0.204 | 0.089 | 0.044 | 0.023 | 0.012 | 0.005 |
| −0.1913 | 0.263 | −0.587 | 0.801 | 0.104 | 0.037 | 0.017 | 0.009 | 0.004 | 0.002 |
| −1.2907 | 0.762 | −0.110 | −0.211 | 0.968 | 0.076 | 0.028 | 0.013 | 0.007 | 0.003 |
| −2.9650 | 1.170 | −0.042 | −0.065 | −0.099 | 0.991 | 0.045 | 0.017 | 0.007 | 0.003 |
| −4.9263 | 1.568 | −0.020 | −0.030 | −0.034 | −0.052 | 0.997 | 0.026 | 0.009 | 0.003 |
| −6.8749 | 1.962 | −0.011 | −0.015 | −0.016 | −0.019 | −0.029 | 0.999 | 0.015 | 0.004 |
| −8.5195 | 2.356 | −0.006 | −0.008 | −0.008 | −0.008 | −0.010 | −0.016 | 0.999 | 0.007 |
| −9.6156 | 2.749 | −0.002 | −0.003 | −0.003 | −0.004 | −0.005 | −0.005 | −0.007 | 0.999 |

(b) "sine" states $\Psi_-^0$

| $E_q^1$ | $k_q^{\text{eff}}$ | $k$: 0.3927 | 0.7854 | 1.1781 | 1.5708 | 1.9635 | 2.3562 | 2.7489 | 3.1416 |
|---|---|---|---|---|---|---|---|---|---|
| −0.3976 | 0.394 | 0.999 | −0.029 | −0.015 | −0.010 | −0.008 | −0.006 | −0.006 | −0.004 |
| −1.5221 | 0.788 | 0.028 | 0.998 | −0.048 | −0.025 | −0.017 | −0.013 | −0.012 | −0.008 |
| −3.1886 | 1.181 | 0.015 | 0.045 | 0.996 | −0.064 | −0.033 | −0.024 | −0.020 | −0.013 |
| −5.1367 | 1.575 | 0.010 | 0.025 | 0.058 | 0.993 | −0.081 | −0.044 | −0.034 | −0.022 |
| −7.0719 | 1.970 | 0.008 | 0.017 | 0.032 | 0.071 | 0.988 | −0.110 | −0.064 | −0.040 |
| −8.7046 | 2.370 | 0.007 | 0.014 | 0.023 | 0.040 | 0.089 | 0.974 | −0.182 | −0.091 |
| −9.7834 | 2.827 | 0.005 | 0.010 | 0.017 | 0.027 | 0.048 | 0.113 | 0.874 | −0.469 |
| −10.2137 | 3.032 | 0.009 | 0.018 | 0.029 | 0.045 | 0.077 | 0.155 | 0.444 | 0.877 |

The exponent $a$ in (21) was taken as 2.0 since this value approximately describes the decay of the $H_{rs}^{j_1 j_2}$ atomic orbital integrals for the carbon atom as calculated [10] by the Wolfsberg–Helmholtz relationship using Slater AOs.

The eigenvalues and eigenvectors of the "sample calculation" with $n = 16$ are shown in Table 3 where the usual 10 eV wide energy band (with minimum at the BZ centre) has been perturbed by a function with amplitude $v' = +1.0$ eV. In terms of the Wolfsberg–Helmholtz–Slater relationship referred to such a perturbation of a pure $\pi$ MO, for example, could describe the *extension* of a C–C segmental link by ~0.1 Å. The spectrum of energy eigenvalues $E_q^1$ and their $k_q^{\text{eff}}$'s for both $\Psi_+^0$ and $\Psi_-^0$-derived cases show quasi-continuous energy levels approximately in the range 0 to −10 eV which are practically equivalent to the microstate energies of the unperturbed band $E^0(k)$. Superimposed on these levels and prominently separated from them, above and below, are the pair at $E_{q*}^1(+) = 0.4019$ and $E_{q*}^1(-) = -10.2137$ eV which are derived from the $\Psi_+^0$ and $\Psi_-^0$ functions respectively. (The effect of increasing $n$ is to pack the range 0 to −10 eV more closely with quasi-continuous levels, leaving the states $E_{q*}^1(+)$ and $E_{q*}^1(-)$ unchanged.)

The eigenvectors show the same features as those discussed in Sect. 3.1 for the $V$ perturbation, reflecting a greater degree of microstate mixing for the discrete states $\Psi_{q*}^1(+)$ which, as we saw, indicated localization at the perturbation site.

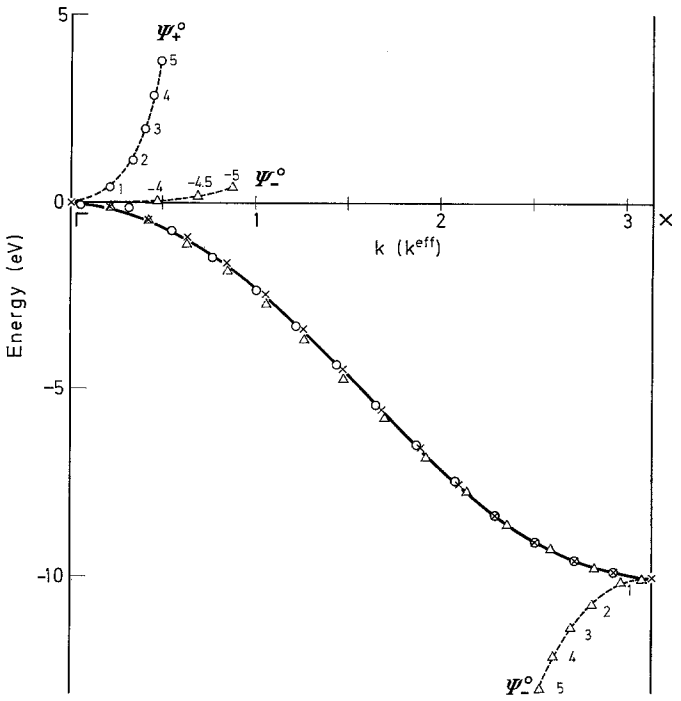


**Fig. 5.** Continuous curve: Undistorted 10 eV energy band $E^0(k)$; Dotted curve: Discrete states generated by $V'$ (Fig. 4) with the amplitudes $v$ shown (−5 to +5 eV). Points denoted ○ are those calculated using $\Psi_+^0$ functions; those shown △ are from $\Psi_-^0$

Figures 5 and 6 respectively illustrate the effects of varying the amplitude $v'$ of the perturbation $V'$ and the width $E_w$ of the energy band and are analogous to Figs. 2 and 3 for the $V$ perturbation. Both positive and negative perturbations are illustrated in Fig. 5 but only the $\Psi_-^0$ functions are found to give rise to discrete states when $v'$ is negative. Probably the $(v'<0)$-generated $\Psi_{q^*}^1(+)$ states would appear for large $|v'|$ (cf. Fig. 2), i.e. for a sufficiently large compression of the selected link, but it was decided to restrict the extent of the distortion to that which is chemically feasible.

In Fig. 6, which demonstrates the variation of the discrete state separations $\varepsilon$ with the width $E_w$ of the energy band only positive perturbations were selected, but in view of our discussion (Sect. 2.3) on the complementarity of the signs of $v'$ and $E_w$ it should be clear that the effect of reversing the sign of $v'$ would be to invert the curves in Fig. 6 through the origin.

## 5. Discussion

In this work a polymer wave function was perturbed at a single site on the chain so simulating a practical feature of the polymer such as a defect or distortion at such a point. The result, a generation of electronic energy states shifted from the energy band by amounts roughly proportional to the perturbation amplitude, consists of a set of energetically sensitive MOs which are

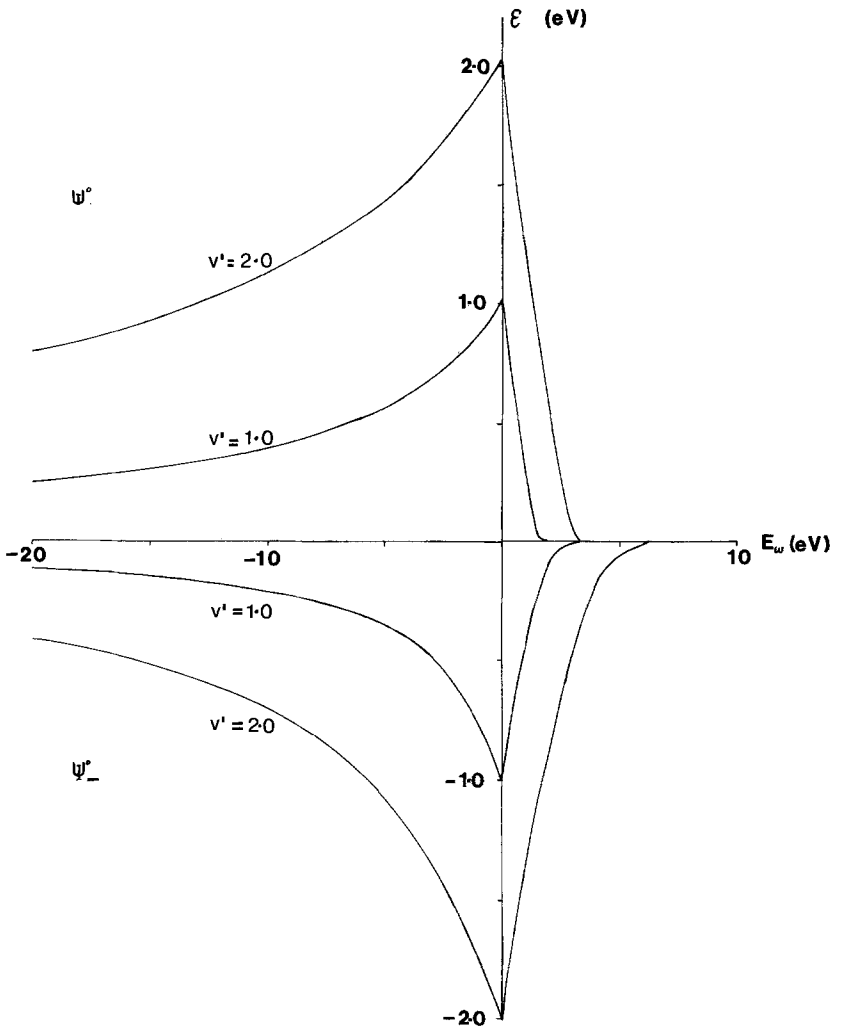


**Fig. 6.** The separation $\varepsilon$ of the "discrete state" energy level from the band $E^0(k)$ as a function of the width $E_w$ of the band, upon application of $V'$

localized in the region of the perturbation. Since oribtals of favourable symmetries and energies play decisive rôles in qualitative [12] and quantitative [13] descriptions of chemical reactivity our results suggest that perhaps we should consider the use of such a perturbation approach to treat some of the features involved in an encounter between a polymer and a reacting species.

The results of the single link distortion perturbation $V'$ of Sect. 4 are qualitatively similar to those of the chain scission perturbation reported in Ref. 4, where discrete states were produced from calculated energy bands in simple hydrocarbon polymers and where, unlike the present case, segmental AO interactions were considered. For a study of chemical reactions, however,

which (at least for hydrocarbon polymers) are much more likely to proceed by a *concerted* process than by a chain rupture followed by a molecular encounter, an approach using a potential such as $V$, which can be made to vary smoothly along the reaction coordinate, is probably more realistic.

## References

1. Born, M., von Kármán, Th.: Z. Phys. **14,** 15 (1913); Bloch, F.: Z. Phys. **52,** 555 (1928); Altmann, S. L.: Band theory of metals (the elements), Chapt. 3. Oxford: Pergamon Press 1970; Levin, A. A.: Solid state quantum chemistry, Chapt. 2. New York: McGraw Hill 1977
2. Koster, G. F., Slater, J. C.: Phys. Rev. **95,** 1167, 1436; *ibid* **96,** 1208 (1954); Zunger, A.: Ann. Soc. Sci. Bruxelles **89,** 231 (1975); McCubbin, W. L.: André, J.-M., Delhalle, J., Ladik, J. (Eds.): The quantum theory of polymers, p. 185; Dordrecht: D. Reidel (1978); Martino, F.: *ibid* p. 169; Del Re, G.: *ibid* p. 199
3. Morton-Blake, D. A.: Intern. J. Quantum Chem. (in press) (1980)
4. Morton-Blake, D. A.: Theoret. Chim. Acta (Berl.) **51,** 85 (1979)
5. Heine, V.: Group theory in quantum mechanics, Chapt. VI. Oxford: Pergamon Press 1960; Quinn, C. M.: Quantum Theory of Solids, Chapt. 2. Oxford: Clarendon 1973
6. Karpfen, A., Petkov, J.: Theoret. Chim. Acta (Berl.) **53,** 65 (1979)
7. Gurman, S. J., Pendry, J. B.: Phys. Rev. Letters **31,** 637 (1973); Feuerbacher, B., Willis, R. F.: J. Phys. C **9,** 169 (1976)
8. Maue, A. W.: Z. Physik **94,** 717 (1935); Goodwin, E. T.: Proc. Cambridge Phil. Soc. **35,** 205, 221, 232 (1939); Statz, H.: Z. Naturforsch. **5a,** 434 (1950); Levine, J. D.: Phys. Rev. **171,** 701 (1968); Phariseau, P.: Physica **26,** 737 (1960); Davison, S. G., Levine, J. D.: Solid state physics, Vol. 25. New York: Academic Press 1970
9. Imamura, A.: J. Chem. Phys. **52,** 3168 (1970); Morokuma, K.: J. Chem. Phys. **54,** 962 (1971); André, J.-M., Delhalle, J.: André, J.-M., Delhalle, J., Ladik, J. (Eds.): The quantum theory of polymers, p. 1. Dordrecht: D. Reidel 1978; André, J.-M., Ladik, J.: Proceedings of the NATO ASI on the electronic structure of polymers and molecular crystals, p. 1, **B9**: Plenum Press, and references therein
10. Wolfsberg, M., Helmholtz, L.: J. Chem. Phys. **20,** 837 (1952)
11. Slater, J. C.: Phys. Rev. **36,** 57 (1930)
12. Woodward, R. B., Hoffman, R.: The conservation of orbital symmetry, Weinheim: Verlag Chemie 1970; Fleming, I.: Frontier orbitals and organic chemical reactions, London: John Wiley and Sons 1976
13. Daudel, R.: Quantum theory of chemical reactivity. Dordrecht: D. Reidel 1973

Received January 28, 1980